Assessing Large Signal Performance of Transducers

W. Klippel
Klippel GmbH
Germany
www.klippel.de

ABSTRACT

Loudspeakers, headphones, shakers and other electromechanical and electroacoustical transducers manufactured today are still analog systems producing substantial distortion at high signal amplitudes. More and more applications require small and lightweight transducers manufactured at minimal cost but producing the acoustical output at sufficient quality. Straightforward measurements based on the linear system theory fail at high amplitudes. New measurement and simulation techniques have been developed for the large signal domain considering nonlinear, thermal and other time-variant mechanisms. Large signal parameters measured by system identification reveal limits and defects of the driver and make numerical prediction of the behavior for any artificial or natural stimulus possible. This information is required for systematic diagnostic and optimal system design considering both objective and subjective constraints.

1   Introduction

Professional, multimedia, automotive and home applications require more and more small, light-weight transducers manufactured at low cost generating the acoustical output at high efficiency and low signal distortion. Here the transducers are used as "loud"-speakers and the performance at high signal amplitudes is very important. There are three ways for assessing the behavior and the quality of the speaker as illustrated in Fig. 1.

The first way uses the human ear to assess the sound quality subjectively. Systematic listening tests are required to provide reliable results. However, the engineer also needs objective data based on physical measurements. At small amplitudes the speaker can be described by a linear system completely characterized by the amplitude and phase response. At medium amplitudes a loudspeaker produces new spectral components. Traditional measurement techniques measure the harmonic and intermodulation distortion for a single-tone or multi-tone stimulus. This data describe only special symptom of the large signal behavior but not the physical cause itself. Loudspeaker research performed in the last decade has provided more accurate models for the loudspeaker system considering nonlinear, thermal and other time-varying mechanisms in the loudspeaker. These results are basis for new powerful tools for measuring loudspeaker parameters valid in the large signal domain, for predicting the nonlinear behavior and investigating the impact on the subjective listening impression. This paper gives a summary on these techniques and performs a practical diagnostics of a example driver.
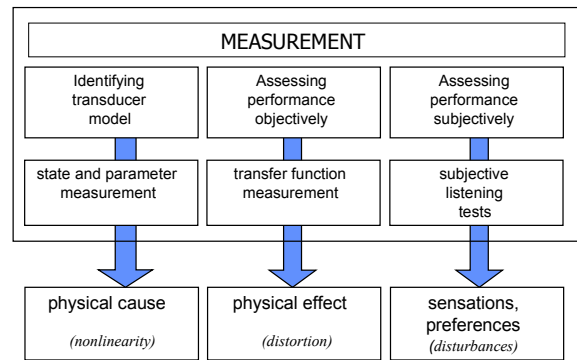
Fig. 1: Ways for assessing loudspeakers

2   Transducer Modeling

Most of actuators used in speakers, headphones and other applications use a voice coil in a static magnet field to generate an electro-dynamical driving force for the electro-mechanical system. For this type of transducer a model is developed which preserves important features of this principle but neglect the properties of the particular unit which are not relevant for the overall performance such as shape, color, material, ...
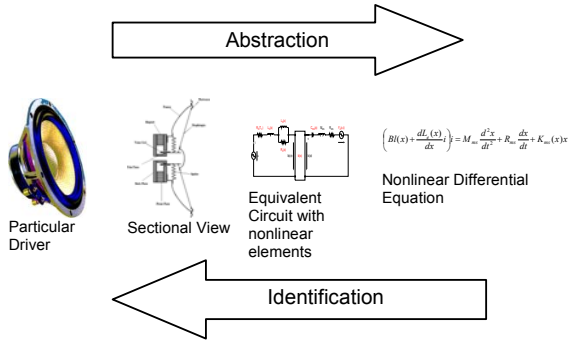
Fig. 2: Modeling of speakers in the large signal domain

Fig. 2 illustrates the abstraction process. At low frequencies where the wavelength is large in comparison to the geometrical dimension the state of a transducer may be described by few variables:

$x(t)$ displacement of the voice coil,
$v(t)$ velocity of the voice coil,
$i(t)$ the electric input current,
$u(t)$ the driving voltage at loudspeaker terminals,
$F_a(t)$ force related to the sound pressure at the diaphragm

The relationship between the state variables may be described by a lumped parameter model comprising a few number of elements characterized by parameter values. The number and kind of the lumped elements and the way how they are connected may be called the topology of our model. It is may be graphically represented as an electrical equivalent circuit as shown in Fig. 3.
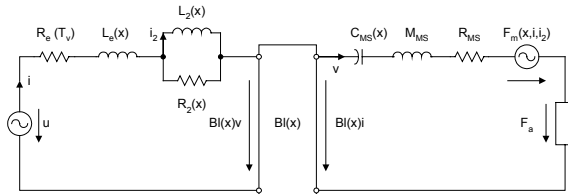
Fig. 3. Electro-mechanical equivalent Circuit

In contrast to the traditional linear model some parameters are not constant but depend on time varying variables such as displacement, current, voice coil temperature T_V.:

$R_e(T_V)$ DC resistance of voice coil,
$L_E(x)$ part of voice coil inductance which is independent on frequency,
$L_2(x)$ para-inductance of the voice coil which vanishes at higher frequencies,
$R_2(x)$ electric resistance due to additional losses caused by eddy currents,
$Bl(x)$ instantaneous electrodynamic coupling factor (force factor of the motor) defined by the integral of the permanent magnetic flux density B over voice coil length l,
$F_m(x,i,i_2)$ reluctance force due to electro-magnetic motor principle,
M_{MS} mechanical mass of driver diaphragm assembly including voice-coil and air load,
R_{MS} mechanical resistance of driver suspension losses,
$C_{MS}(x,t)$ mechanical compliance of driver suspension (the inverse of stiffness $K_{MS}(x,t)$.

3   Identification of the Driver Model

The large signal model of the speaker comprises structural information, free parameters and state variables. The tools becomes most powerful if we apply the theory to a real driver in the real world. This is called the identification process which is just the opposite of the abstraction as illustrated in Fig. 2.

The first task is to prove that the topology is adequate for the type of transducer and the principle of conversion used. The second task of the model identification is to specify the free parameters of the model for the particular unit. In the third step all of the state variables and the output signal may be predicted for any input signal using an adequate topology and optimal parameters.
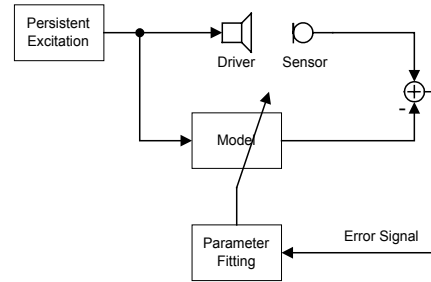
Fig. 4. Identification of the driver model

The identification of model may be accomplished by static, quasi-static or dynamic techniques. Only the full dynamic technique as shown in Fig. 4 can measure the transducer under normal working condition. The speaker is persistently excited by a broad band signal such as noise or an ordinary music signal. At least one electrical, mechanical or acoustical signal has to measured simultaneously. Monitoring the electric input current at the terminals and detection of the back EMF gives a signal proportional to the voice coil velocity and dispenses with an expensive sensor.

Connecting the model in parallel to the driver/sensor system the agreement between driver and model may be evaluated by an error signal which is the difference between measured and predicted output. The parameters may be adaptively adjusted to optimal estimates by reducing the amplitude of the error signal with a LMS-algorithm.

Implementing this approach in a digital system (DSP) we may measure the parameters and state variables on –line [13 – 14]. An error signal of low amplitude proves that the model topology is adequate and optimal estimates on the parameters are found. Reversible and non-reversible changes of the parameters, thermal processes and destruction and malfunction may be monitored and investigated versus time.

3.1   Large Signal Parameters

The Large Signal Identification has been applied to a example drivers which has been intended for high-quality applications.

Parameters	Driver A	Unit
f_s	30.5	Hz
$Bl(x=0)$	7.43	N/A
$C_{MS}(x=0)$	1.28	mm/N
$Le(x=0)$	0.47	mH
L_2	0.32	mH
M_{MS}	21.1	g
Q_{MS}	2.87	
R_2	2.18	Ohm
R_E	3.54	Ohm

Table 1. Parameters at the rest position

The example driver is an 8 inch woofer with a relatively high force factor as shown in Table 1. This corresponds with a short voice coil overhang causing an early decay of the *Bl*-product at small displacement as shown in Fig. 5.
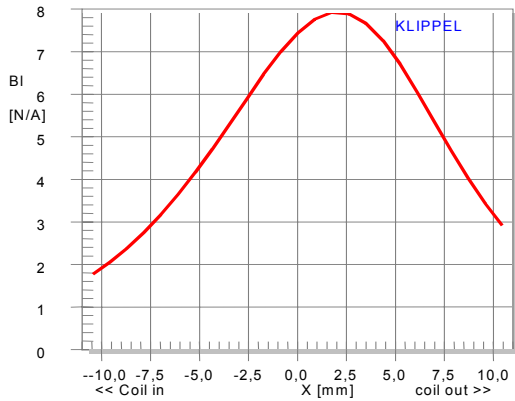
Fig. 5. Force factor *Bl(x)* versus displacement *x* of Driver A

The voice coil height corresponds approximately with the peak to peak displacement of 14 mm where the instantaneous force factor value decays to 50% of the maximal value. The rest position of the coil is not in the Bl-maximum producing a significant asymmetry in the curve.
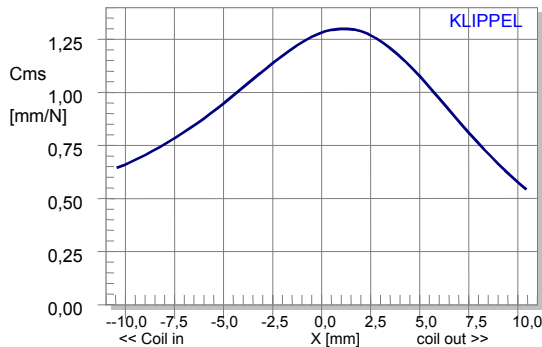
Fig. 6. Compliance $C_{ms}(x)$ versus displacement x of Driver A

Whereas the capability of the motor is almost exhausted at x = - 9 mm the compliance of the suspension decreases only down to 44% as shown in Fig. 6. Most suspensions handle a variation of $C_{ms}(x)$ down to 20 % without causing any damage. The maximum of the compliance is not at the rest position but for higher positive displacement the compliance decreases faster than for negative displacement giving almost the same compliance at x = +- 7 mm. Thus, the symmetry of the suspension is quite acceptable.
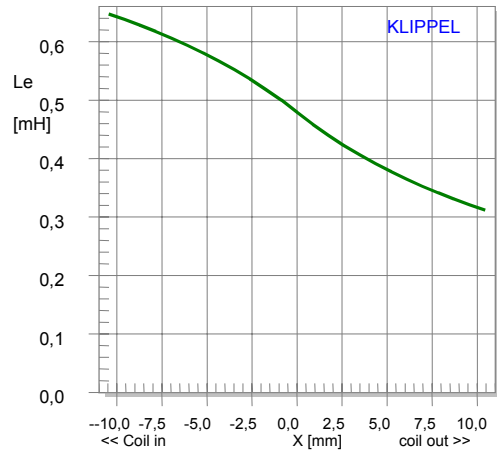
Fig. 7. Inductance versus displacement x of Driver A

The voice coil inductance $L_e(x)$ as shown in Fig. 7 has a distinct asymmetrical shape increasing when the coil is moving towards the back plate. This is typical for drivers using no short cut ring or other means for reducing the voice coil inductance.
The nonlinear curves may be developed into a power series expansion. Thus the whole driver may be represented by few numbers which have a physical meaning.

4   Identification of State Variables and Output Signal

Providing an input signal (voltage) to the driver terminals the state variables (displacement) and the output signal (sound pressure) describe as the behavior of the speaker. In this chapter we discuss traditional to measure these signals directly and new techniques which provide this signals without any sensor.

4.1   Direct Measurement
The measurement of the state variables and the output signal as illustrated in Fig. 8 is the most simple way for assessing the transfer behavior.

Fig. 8. Measurement of the transfer response

Measurements of electrical current and sound pressure can be accomplished with normal equipment. The measurement of the displacement requires a special sensor but an inexpensive laser based on triangulation becomes more and more an indispensable tool for driver development. For the measurement of the air velocity in the port a hot-wire anemometer is usually not available.

4.2   Prediction

Having an adequate model topology and valid parameters for the particular driver and enclosure we may predict the state variables for any input signal u(t) by numerical as illustrated in Fig. 9.
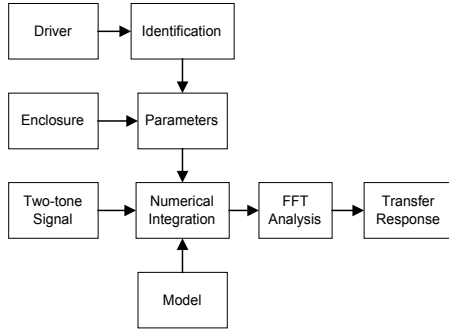
Fig. 9. Prediction of the Transfer Response

Comparing the predicted response with the response based on easy to do electrical current or sound pressure measurements is a simple test to prove that the modeling is valid and the parameters are reliable. Then the measurements of other variables requiring special sensors may be replaced by numerical predictions.

4.3   Simulation

Whereas the prediction uses the parameters of a real loudspeaker system we may also simulate the behavior of a virtual loudspeaker before the first prototype has been finished. The parameters may be produced by FEM-calculations or by simply modifying the parameters of an existing speaker to assess design choices as illustrated in Fig. 10.
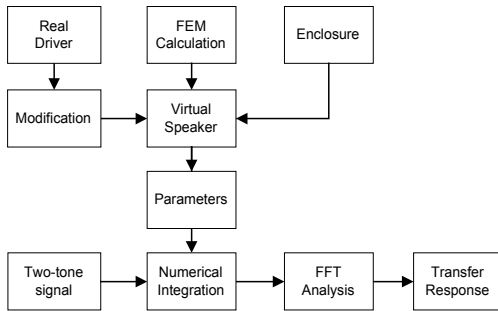
Fig. 10. Simulation of the transfer response

To investigate the effect of each nonlinearity separately and to find the dominant source of distortion the following nonlinearities might be switched on and off during simulation:

- motor nonlinearity due to $Bl(x)$
- mechanical suspension nonlinearity due to $C_{ms}(x)$
- inductance nonlinearity due to $L_e(x)$
- para-inductance nonlinearity due to $L_2(x)$
- losses from eddy currents due to $R_2(x)$
- reluctance force (electromagnetic drive)
- adiabatic compression in enclosure $C_{AB}(P_{box})$
- adiabatic compression of rear enclosure $C_R(P_{rear})$
- radiation distortion (Doppler effect)

Clearly modifying the large signal parameters will create a new virtual driver with a different behaviour in the large signal domain.

4.4   Auralization

Auralization is a new technique to investigate the effect of the separated distortion component in the output signal. The Auralization is also based on a nonlinear speaker model as shown in Fig. 11 implemented in digital signal processor to calculate all state variables in real time. An audio signal (music) or any artificial test signal may be use as signal source via an AD-converter. In contrast to the simulation the output signal is decomposed into a linear signal p_{lin} and the nonlinear distortion p_B, p_C and p_L generated from the separated nonlinearities force factor Bl(x), Compliance $C_{ms}(x)$ and inductance $L_e(x)$, respectively. A mixing console sums the weighted signal components and generates at the output the output $p_{out}(t)$ for headphone and loudspeaker reproduction. The user may attenuate each signal components to listen to each distortion components and any ratio between distortion and the linear signal. Systematic listening test based on blind AB-comparison may be performed to predict the threshold of audibility depending on properties of the signal and speaker. Simultaneously the all of the state variables (displacement, voltage, current, power, temperature, sound pressure) and the peak value of distortion are monitored in real time. This technique combines subjective and objective evaluation techniques.
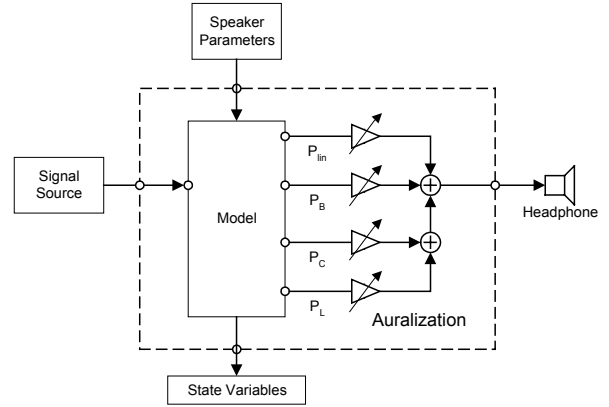
Fig. 11: Digital speaker simulation in real time (Auralization)

5   Large Signal Behavior

Clearly the behavior of the transducer depends on the spectral and temporal properties of the input signal. In this chapter we investigate the behavior of speaker for different stimuli and their relationship to the large signal parameters.

5.1   Two-Tone Excitation Signal

The traditional measurement technique as recommended in the standard IEC 60268 use a single or a two-tone excitation signal defined by

$$u(t) = U_1 \sin(2\pi f_1 \cdot t) + U_2 \sin(2\pi f_2 \cdot t) \tag{1}$$

This artificial stimulus has some advantages. Performing an FFT analysis of the state variables or the output signal we find in addition to the fundamental frequencies f_1 and f_2 distortion components which may be easily interpreted as fundamental, DC-component, harmonic, sub-harmonic, difference-tone and summed-tone intermodulation distortion as shown in Fig. 12.
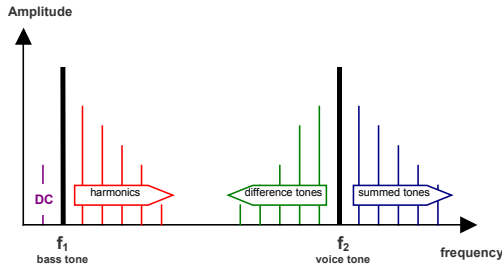
Fig. 12. Spectrum of sound pressure signal of a two-tone excitation signal (bold lines) and distortion components (thin lines)

The frequencies f_1 and f_2 and the amplitude U_1 and U_2 may be varied to perform frequency and amplitude sweeps. Different methods are recommended in the standard IEC 60268. The measurement of the harmonic and modulation distortion gives most informative data about the speaker. The first tone f_1 is set below or close to the resonance frequency f_s representing a bass component that produces significant voice coil displacement. The second tone f_2 represents any audio component (voice) in the pass band of the transducer.

The driver variables in steady state condition are subject to a FFT analysis. The amplitude of the spectral component may be displayed versus frequency and voltage. At higher amplitudes the nonlinearities inherent in the speaker will produce a non-trivial relationship between input and output amplitude.
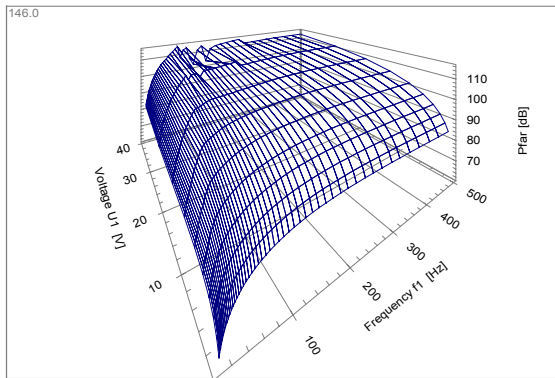
Fig. 13: Simulated sound pressure response of the fundamental component versus terminal voltage U_1 and excitation frequency f_1.

5.1.1 Fundamental Component

Fig. 13 shows the SPL of fundamental component reproduced by the example speaker versus frequency f_1 and amplitude U_1 of a single-tone stimulus. This 3D plot revels a distinct amplitude compression at high amplitudes for low frequencies.

The fundamental response in the voice coil displacement for a single excitation tone varied versus frequency and amplitude is shown in Fig. 14.
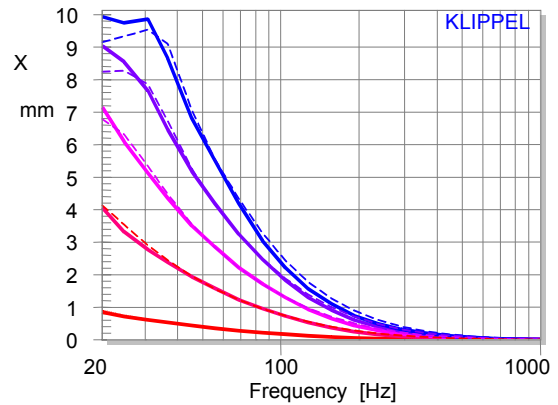
Fig. 14. Fundamental displacement x of Driver A predicted (bold lines) and measured (thin line) at peak voltage U = 1, 4.5, 8, 11.5, 15V

Five frequency sweeps are performed at different amplitudes of input voltage u(t) linearly increased from 1 to 15 V by 3.5 V steps. The predicted curves (bold lines) agree quite well with the thin curves measured by using a laser displacement meter. Both measured and predicted curves reveal an amplitude compression. Whereas the first amplitude step increases the peak displacement by 3 mm there is only an increase about 1 mm in the last step. The linear model would predict a maximal amplitude of 13 mm at U=15 V.

5.1.2 DC-Component

A loudspeaker with asymmetrical parameters will rectify an AC-signal producing a DC-component in the displacement dynamically. Fig. 15 shows the predicted and measured DC-displacement in comparison to the fundamental component of 70 Hz versus input voltage.

The DC part of the displacement is in the same order of magnitude as the AC component. This is due to the asymmetrical Bl(x) characteristic which causes an instability of the driver. At frequencies above resonance $f > f_s$ the coil will slide down on the slope of the $Bl(x)$-curve and will be literally pushed out of the gap dynamically.
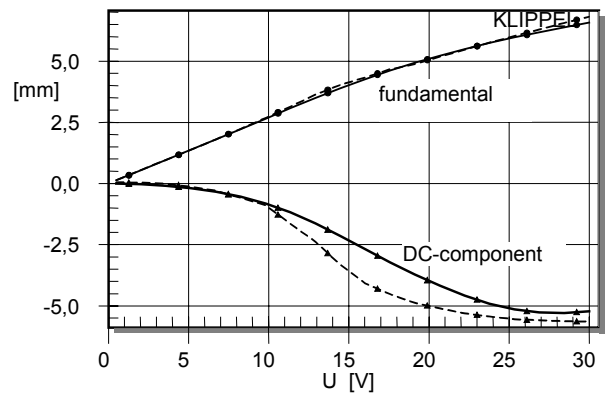
Fig. 15. Fundamental (circle) and DC-part (triangle) in voice coil displacement versus input voltage of excitation tone at f=70 Hz measured (thin line) and predicted (bold line).

Only the stiffness of suspension will produce an opposite force keeping the coil in the gap. Clearly, a suspension with higher stiffness and nonlinear characteristic will   reduce the DC-displacement but also any AC-component. However, changes on the suspension will reduce the effect but does not remove the cause of the instability. This problem may be easily fixed by correcting the rest position of the coil.

5.1.3   Harmonic Distortion

The total harmonic distortion in the radiated sound pressure signal predicted and measured for a sinusoidal voltage signal with $U_{peak}=$ 1 V, 8 V and 15 V are shown in Fig. 16.
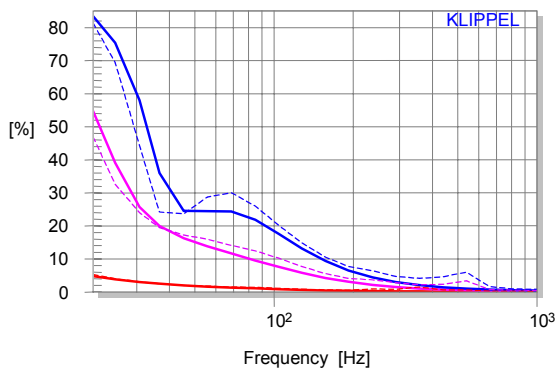
Fig. 16. Total harmonic distortion of Driver A measured (dashed line) at U = 1V, 8V, 15 V and predicted (bold line) from large signal parameters

Below the resonance frequency the energy of the harmonics dominates the sound pressure output. Expressing the distortion in percent according to IEC 60268-5 we get more than 80 % for the example driver. This is a general phenomenon caused by a couple of reasons:

- the amplitude of the displacement is high for $f < fs$ producing substantial parameter variation due to $L_e(x)$, $C_{ms}(x)$ and $Bl(x)$-nonlinarities,
- the input current has a high value and is in phase with the displacement producing high motor distortion,
- fundamental component is below the cut-off frequency but the harmonic will still be radiated in the pass-band .

At higher frequencies the total distortion gradually decreases to small values below 1%.
A detailed analysis of the spectral component of the second- and third order shows the relationship to the nonlinear parameters.
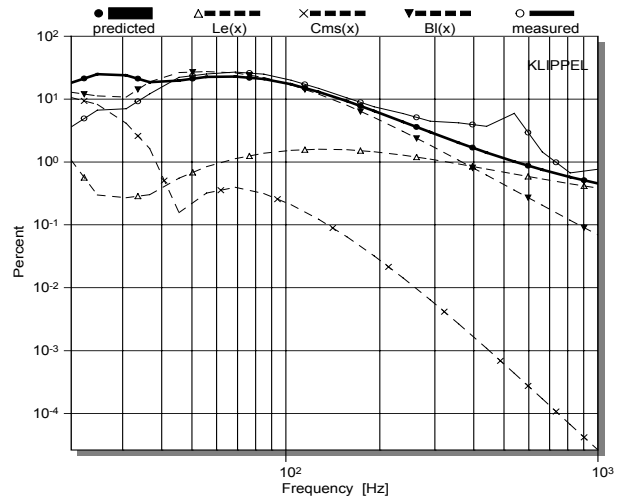
Fig. 17. Second-order harmonic distortion of Driver A measured (thin line) and predicted considering all nonlinearities (bold line) and separated nonlinearities (dashed lines)

Fig. 17 shows the measured and predicted second-order distortion as thin and bold curve, respectively. The good agreement confirms that the modeling is quite reliable and we may use the numerical tool for simulations of driver modifications. Considering only one nonlinearity while replacing all of the remaining parameters by the corresponding constant value from the rest position shows the effect of each nonlinearity separately.

The asymmetry of the $Bl(x)$-nonlinearity is the dominant source of second-order distortion represented as dotted line with downward triangles because this curve is close to the measured and predicted response considering all nonlinearities. The asymmetry of the suspension causes 10 % distortion below the resonance frequency but decreases at a rate of 24 dB /octave to higher frequencies. The second-order harmonics produced by inductance $L_e(x)$ and Doppler distortion are negligible.

If we measure only harmonic distortion we will find usually very low values of harmonic distortion in the passband of the driver. However, the low harmonics does not ensure that the speaker does behave well for a more complex input signal.

5.1.4   Intermodulation Distortion

Distortion measurements using a single sinusoidal tone can not reflect intermodulation between components in the audio signal. A simple two tone signal comprising a variable tone f_1 and a second tone with constant frequency f_2 =70 Hz shows the nth-order intermodulation components at difference frequencies $f_1 - nf_2$ and summed frequencies $f_1 + nf_2$ for $n=1,2,...$ Fig. 18 shows the second-order intermodulation ($n=1$) in the radiated sound pressure according IEC 60268-5 for the example driver.
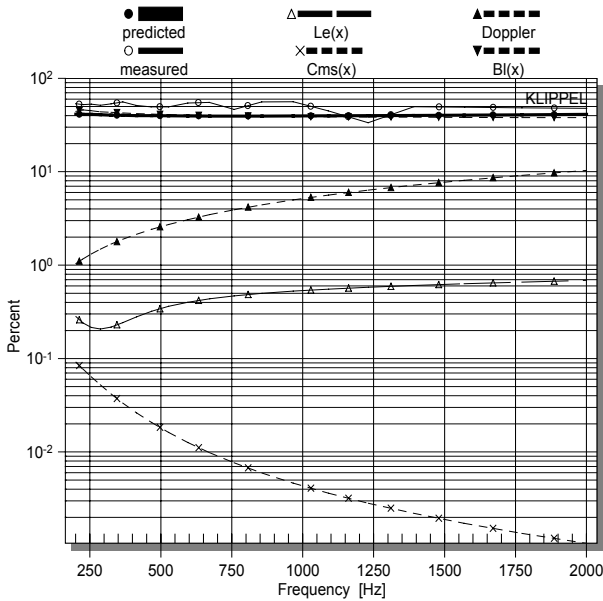
Fig. 18. Second-order intermodulation of Driver A measured (thin line) and predicted considering all nonlinearities (bold line) and separated nonlinearities (dashed lines)

Both the measurement and the prediction agree in substantial distortion which is constant at about 40%. This is typical for motor distortion caused by an asymmetry in the *Bl(x)-curve*. Intermodulation distortion of this magnitude is clear audible as a roughness of the high-frequency component.

The intermodulation due to the *Le(x)* nonlinearity are at a constant level of 1 % at higher frequency. The Doppler distortion increase by 6dB/octave to higher frequencies and come up to 10 % for f_1= 2kHz. The intermodulation distortion from $C_{ms}(x)$ are less than 0.1% at very low frequencies and may be neglected at higher frequencies.

5.2   Multi-tone Excitation Signal

Increasing the spectral complexity of the excitation signal will produce a multitude of harmonic and intermodulation components due to all combinations of the fundamental tones. Fig. 19 shows the spectrum of a sound pressure signal generated by multi-tone signal with equally spaced lines of the same amplitude. It is important that the excitation spectrum is sparse that means not all frequencies are excited. At these frequencies the nonlinear distortion can be detected. There are many interferences and the harmonics can not be distinguished from summed-tone and difference-tone intermodulation. Performing an additional measurement without excitation signal we can measure the noise floor from ambience sound.
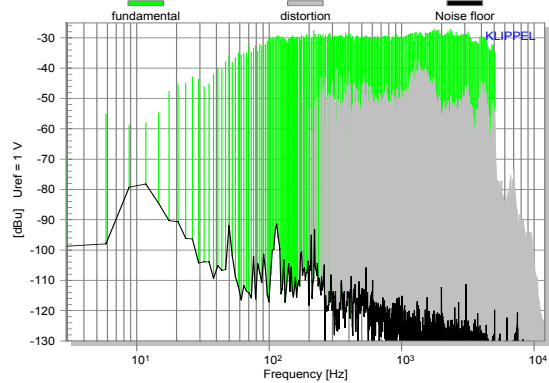
Fig. 19: Sound pressure spectrum of a reproduced multi-tone signal

There is an almost constant distance of about 15 dB between fundamentals and distortion components for the example speaker shown in Fig. 19. Again we see that the asymmetry of the force factor generates high amount of distortion (> 20 %) when a low frequency bass tone with high displacement modulates any high frequency voice tone. It is typical for this kind of speaker distortion that the intermodulation are close to the voice tone. Above 5 kHz where the multi-tone signal provides no excitation the driver produces much less distortion (< 1 %) because only harmonics and summed-tone intermodulation between high-frequency fundamentals are generated. Again we see that the harmonics are not the most critical distortion in loudspeakers.

The other speaker nonlinearities such as $C_{ms}(x)$, $L_e(x)$, Doppler effect will produce characteristic shape of the distortion floor which might be useful fingerprint of used for speaker diagnostics.

5.3   Testing with Music

The Auralization technique makes it possible to investigate the calculate the state variables and the separated distortion components on-line for any input signal (music, speech, test signals).

The behavior of the example driver is investigated with three pieces of music (from the CD "Fast Car" by T. Chapman):

Piece	time	Title	Track	Properties
1	0 ... 300 s	Baby can I hold you	5	large displacement
2	300... 600s	Behind the wall	4	mainly voice
3	600... 900s	Mountains o'things	6	very low frequencies

The three tracks differ in spectral signal properties. Fig. 20 shows the input power P and the voice coil temperature T_V versus measurement time t. Due to the high efficient motor used in the example driver the heating of the coil and the thermal power compression is negligible.
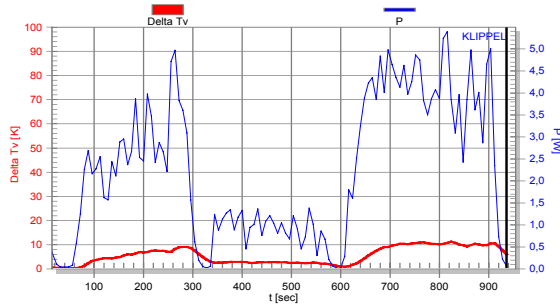
Fig. 20: Real input power P (thin line) and voice coil temperature T_V (bold line) during the Auralization

Clearly, the second piece with the solo voice provides the lowest input power P and generates only low voice coil displacement as shown in Fig. 21. The first piece produces maximal voice coil displacement of almost 10 mm. Here we find a DC component generated dynamically that pushes the voice coil more than 1 mm in negative direction.
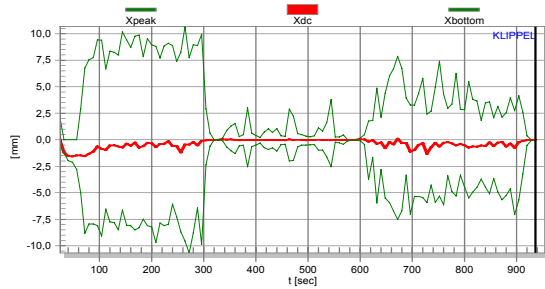
Fig. 21: Maximal positive and negative displacement X_{peak} and X_{bottom} and DC-component X_{DC} (bold line) during Auralization.

Fig. 22 shows the contribution of each nonlinearity as the ratio of the peak value of the distortion referred to the total sound pressure output. Clearly, the force factor is the dominant source of distortion for all the three music examples. It exceeds 60 % in the first piece where the peak displacement is about 10 mm. The distortion from the voice coil inductance are about 20 % in first and third music piece but less than 10 % for the second piece. The nonlinear suspension produces more than 15 % distortion in during the first piece, less than 0.1 % during voice section and about 2 % distortion during the last music piece.
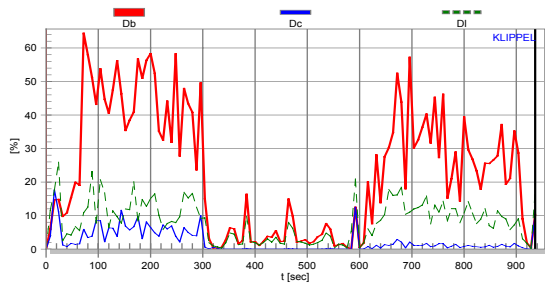
Fig. 22: Peak value of instantaneous distortion d_B, d_C and d_L generated by force factor (thick line), suspension (thin line) and

inductance (dashed line).

The distortion and state variables are the objective output of the auralization. At the same time systematic listening test can be performed to assess the impact on sound quality. The high intermodulation distortion can easily detected in the roughness of the reproduced voice when a bass tone generates high displacement. Most listeners will not be satisfied with the performance of the example drivers at high amplitudes.

6   Remedy for the Driver
Based on the detailed diagnostic of the example driver we can draw conclusions for practical improvements.

A shift of 2 mm in positive direction (coil out) is required for bringing the coil into the Bl-maximum and obtaining a symmetrical characteristic. This is a most effective action which can easily be accomplished and does not affect costs, weight and size of the driver but gives more sensitivity, more stable behavior and less distortion.
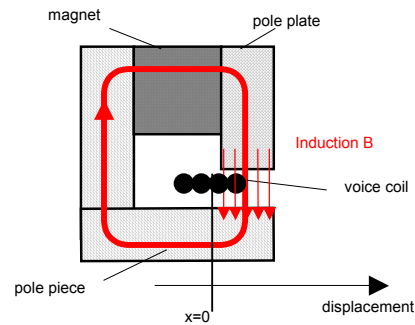
Fig. 23: Offset in rest position of the voice coil

The numerical simulation shows the improvement in performance for the driver fixed virtually. Using a shifted Bl(x) curve and all of the other parameters of Driver A we calculated the second- and third-order distortion in Fig. 24.
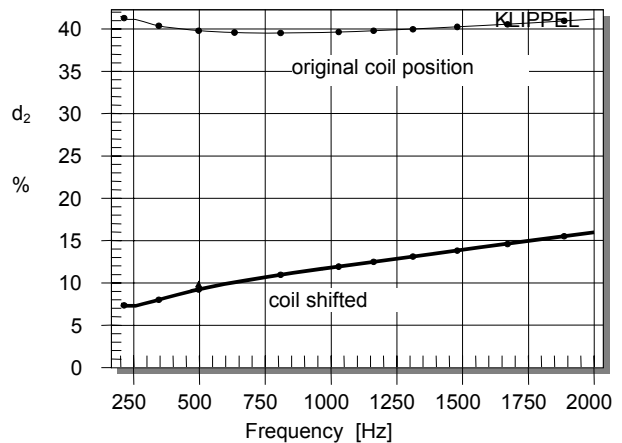
Fig. 24. Intermodulation distortion before (dotted lines) and after (bold lines) correction of the voice coil offset

The second-order distortion can be reduced by 12 dB limited now by Doppler distortion which can be easily identified by a rising slope of 6 dB/octave.

The suspension of example driver needs not much attention because the stiffness curve is sufficiently symmetrical and the

useable working range defined by suspension extends the capability of the motor defined by the coil height.

A short cut ring is not required because the Doppler distortion is almost 20 dB higher than the intermodulation caused by the inductance nonlinearity $L_e(x)$.

7 Conclusion

Extended loudspeaker modeling open new ways for describing and understanding the behavior of loudspeakers in the large signal domain. New measurement techniques have been developed for measuring not only effects and symptom but also to measure the physical causes of the signal distortion expressed as a set of large signal parameters. Each linear, nonlinear and thermal parameter can easily interpreted and is the basis for speaker diagnostics. This information are not only crucial for driver optimization but also for the loudspeaker system design relying on the meaningful driver specifications. A new auralization technique make it possible to combine subjective and objective evaluation used by engineers and marketing people. This is important for defining the target of a speaker more clearly and to develop products with optimal performance, cost, weight, size and in shorter time. The new tools also enable quality control to find defects, reduce number of rejects and manufacture products more consistently.

8 References

[1] R. H. Small, „Direct-Radiator Loudspeaker System Analysis,“ J. Audio Eng. Soc., vol. 20, pp. 383 – 395 (1972 June).

[2] R.H. Small, „Closed-Box Loudspeaker Systems, Part I: Analysis,“ J. Audio Eng. Soc., vol. 20, pp. 798 – 808 (1972 Dec.).

[3] A. N. Thiele, „Loudspeakers in Vented Boxes: Part I and II,“ in Loudspeakers, vol. 1 (Audio Eng. Society, New York, 1978).

[4] D. Button, "A Loudspeaker Motor Structure for Very High Power Handling and High Linear Excursion," J. Audio Eng. Soc., vol. 36, pp. 788 – 796, (October 1988).

[5] C. A. Henricksen, "Heat-Transfer Mechanisms in Loudspeakers: Analysis, Measurement, and Design," J. Audio Eng. Soc., vol. 35, pp. 778 – 791, (October 1987).

[6] E. R. Olsen and K.B. Christensen, "Nonlinear Modeling of Low Frequency Loudspeakers - a more complete model," presented at the 100th convention Audio Eng. Soc., Copenhagen, May 11-14, 1996, preprint 4205.

[7] M.H. Knudsen and J.G. Jensen, "Low-Frequency Loudspeaker Models that Include Suspension Creep," *J. Audio Eng. Soc.,* vol. 41, pp. 3 - 18, (Jan./Feb. 1993).

[8] A. Dobrucki, "Nontypical Effects in an Electrodynamic Loudspeaker with a Nonhomogeneous Magnetic Field in the Air Gap and Nonlinear Suspension," *J. Audio Eng. Soc.,* vol. 42, pp. 565 - 576, (July./Aug. 1994).

[9] A. J. M. Kaizer, "Modeling of the Nonlinear Response of an Electrodynamic Loudspeaker by a Volterra Series Expansion," *J. Audio Eng. Soc.*, vol. 35, pp. 421-433 (1987 June).

[10] W. Klippel, "Nonlinear Large-Signal Behavior of Electrodynamic Loudspeakers at Low Frequencies," *J. Audio Eng. Soc.* , vol. 40, pp. 483-496 (1992).

[11] J.W. Noris, "Nonlinear Dynamical Behavior of a Moving Voice Coil," presented at the 105th Convention of the Audio Engineering Society, San Francisco, September 26-29, 1998, preprint 4785.

[12] D. Clark, „Precision Measurement of Loudspeaker Parameters,“ *J. Audio Eng. Soc.* vol. 45, pp. 129 - 140 (1997 March).

[13] W. Klippel, "Measurement of Large-Signal Parameters of Electrodynamic Transducer," presented at the 107th Convention of the Audio Engineering Society, New York, September 24-27, 1999, preprint 5008.

[14] W. Klippel, "Distortion Analyzer – a New Tool for Assessing and Improving Electrodynamic Transducer," presented at the 108th Convention of the Audio Engineering Society, Paris, February 19-22, 2000, preprint 5109.

[15] W. Klippel, "Diagnosis and Remedy of Nonlinearities in Electro-dynamical Woofers ," presented at the 109th Convention of the Audio Engineering Society, Los Angeles, September 22-25, 2000, preprint 5261

[16] W. Klippel, "Assessment of Voice Coil Peak Displacement X_{max}," presented at the 112th Convention of the Audio Engineering Society, 2002 May 10–13, Munich, Germany.

[17] W. Klippel, "Speaker Auralization – Subjective Evaluation of Nonlinear Distortion," presented at the 110th Convention of the Audio Engineering Society, Amsterdam, May 12-15, 2001, preprint 5310.

[18] W. Klippel, U. Seidel, "Fast and Accurate Measurement of Linear Transducer Parametrs," presented at the 110th Convention of the Audio Engineering Society, Amsterdam, May 12-15, 2001, preprint 5308.

[19] W. Klippel, "Prediction of Speaker Performance at High Amplitudes, "Presented at the 111th Convention of the Audio Engineering Society, 2001 September 21–24, New York, NY, USA, preprint 5418.